

where $H(\hat{R}) = -\sum_i p_i \log p_i$ with $p_i = \langle \Phi_i | \rho | \Phi_i \rangle$, and $c = \max_{i,j} \{ |\langle \Phi_i | \psi_j \rangle|^2 \}$ denotes the maximal overlap for \hat{R} and \hat{S} , where $|\Phi_i\rangle$ and $|\psi_j\rangle$ represent the eigenstates of \hat{R} and \hat{S} , respectively. According to the conjecture from Kraus [7], Maassen and Uffink [4] came up with a simpler result

$$H(\hat{R}) + H(\hat{S}) \geq \log_2 \frac{1}{c}. \quad (2)$$

In practice, there is another scenario that the measured particle is correlated with another. Thus, one raises a fundamental question: whether some new implications and uncertainty relation exist in this case. With this in consideration, Renes *et al.* [8] and Berta *et al.* [9] have proposed and demonstrated the so-called quantum-memory-assisted EUR (QMA-EUR) [10], expressing by

$$H(\hat{R}|B) + H(\hat{S}|B) \geq H(A|B) + \log_2 \frac{1}{c}, \quad (3)$$

where $H(\Lambda|B) = H(\rho_{\Lambda B}) - H(\rho_B)$ with $\Lambda \in (\hat{R}, \hat{S})$ denotes the von Neumann conditional entropy [11], and $H(\rho) = -\text{Tr}(\rho \log \rho)$. The post-measurement state is given by

$$\rho_{\hat{R}B} = \sum_i (|\psi_i\rangle_A \langle \psi_i| \otimes I_B) \rho_{AB} (|\psi_i\rangle_A \langle \psi_i| \otimes I_B), \quad (4)$$

where I_B is the identity operator in the Hilbert space of particle B . This relation can be interpreted by the celebrated uncertainty game. There are two legitimate players (Alice and Bob) who agree on implementing two measurements, \hat{R} and \hat{S} in advance. Bob prepares a pair of entanglements consisting of A and B , and then he transmits A to Alice and keeps B as a quantum memory. Alice makes a measurement on A by choosing one of the observables \hat{R} and \hat{S} after receiving the particle. In final, Bob is capable of predicting Alice's measurement outcome with a minimal uncertainty after Alice informs Bob of her measurement's choices. Remarkably, one can accurately predict the measured outcomes when A and B are maximally entangled. Afterwards, QMA-EUR has been extended to a new form [12–14], and to date some other optimal results have been derived [15–40].

During observing the statistical theory of state and phase transition equations, Lee and Yang proved that the partition functions of thermal systems have zero roots on the complex plane of fugacity or a magnetic field, called Lee–Yang zeros. They provided an insight into the thermodynamic properties of Ising iron magnets at any temperature as well as at any non-zero external fugacity or magnetic field [42, 43]. As a cornerstone of statistical mechanics, they revealed that under very ordinary conditions, all Lee–Yang zeros of a general Ising iron magnet lie on the unit circle of the complex plane, in what is known as the unit circle theorem. Upon

the theorem, in the thermodynamic limit, Lee–Yang zeros form a continuous ring in the complex plane. Beyond the critical temperature, the continuum ring breaks and there is a gap around the positive real axis, which is the exclusion zone for the partition function root, in other words, the free energy is analytical and there is no phase transition. Besides, as the temperature decreases, the gap gradually shrinks, and the two edge points approach the real axis at the critical temperature [42]. Later on, Fisher [44] proposed the concept of Lee–Yang edge singularity where the two edge points [45] of the broken ring are singular. Wei and Liu [46] found that the relationship between Lee–Yang zeros and zero in probe spin coherence coupled to a many-body system is bijective [47, 48]. Moreover, the coherent quenching and birth occurring at the critical time correspond to the Lee–Yang singularity in the thermodynamic limit when the temperature exceeds the critical point.

Through the Lee–Yang zeros point, we can obtain various thermodynamic properties of the system, which is of great significance for examining the phase transition of many-body systems. In addition, QMA-EUR has received much attention because of its critical potential applications in the context of quantum information processing [41], however, a quantum system is susceptible to its surrounding environments in the real world, and then inevitably results in decoherence effects [49]. Till now, one had proposed two different types of Lee–Yang dephasing channels where the partition functions vanish at Lee–Yang zeros, studied the spin squeezing and the concurrence [50]. Nevertheless, there are few investigations on QMA-EUR in Lee–Yang dephasing channels. With this in mind, we focus on how the dephasing channels including the analogous partition function affect the measured uncertainty in reality. In this work, we find that the dephasing channels have a negative effect on the uncertainty, and the analogous partition function is anti-correlated with the uncertainty. Besides, we put forward a working methodology to manipulate the magnitude of the uncertainty by means of the \mathcal{PT} -symmetric operations.

The outline of this paper is structured as follows. In Section 2, we introduce the Lee–Yang zeros and two types of Lee–Yang dephasing channels. In Section 3, we explore the dynamics of the uncertainty under Lee–Yang dephasing channels. Using the \mathcal{PT} -symmetric operation to reduce the entropic uncertainty in Section 4. Finally, we summarize our paper with a brief conclusion in Section 5.

2 Lee–Yang zeros and two types of Lee–Yang dephasing channels

Given a general Ising model with ferromagnetic interactions under a magnetic field h . The Hamiltonian [46] is

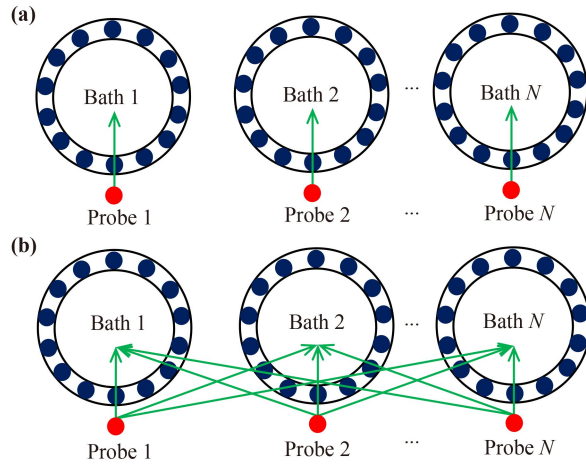


Fig. 1 Two different dephasing channels under a probe(s)-bath system. **(a)** N dephasing channels where probes are only respectively coupled to their own bath. **(b)** The dephasing channel where N probes are coupled to one bath together. The red circles mark probes and the blue circles mark bath spins.

$$H_0(h) = - \sum_{i,j} J_{ij} s_i s_j - h \sum_j s_j, \quad (5)$$

where the spins $s_j = \pm 1$ and the interactions $J_{ij} \geq 0$. The partition function of N_b spins at temperature T can be written as an N -th order polynomial of $z \equiv \exp(-2\beta h)$ as

$$Z(\beta, h) = \text{Tr}[e^{-\beta H}] = e^{\beta N_b h} \sum_{n=0}^{N_b} f_n z^n, \quad (6)$$

where $\beta = 1/T$ is the inverse temperature (Boltzmann and Planck constants are chosen as unity) and f_n is the partition function with zero magnetic fields under the condition that n spins are in the state of -1 . One can calculate its partition function if one wants to understand the physical properties of an exotic system. The N_b zeros of the partition function, which lie in the complex plane of z , form a unit circle, can be written as $z_n \equiv \exp(i\phi_n)$ with $n = 1, 2, \dots, N_b$. As a matter of fact that the Lee–Yang zeros (z_n) only depend on the particle number (N_b) and the temperature (β or $1/T$). If the Lee–Yang zeros are determined, the partition function can be expressed as

$$Z(\beta, h) = f_0 e^{\beta N_b h} \prod_{n=1}^{N_b} (z - z_n). \quad (7)$$

According to Ref. [50], we know that two different types of Lee–Yang channels and probe(s)-bath system whose ferromagnetic Ising bath is under zero field constitutes a typical Lee–Yang dephasing channel. Now we will explain them briefly, for two different types of Lee–Yang dephasing channels in Fig. 1, one is that the probe is only coupled to its own bath, the other one is

the dephasing channel has N probes collectively coupled to one bath. Next, one can apply spin squeezing to dephasing channels, via the advantage of spin squeezing. In order to utilize exchange symmetry, by choosing the one-axis twisted state with an ensemble of N spin-1/2 probes of the ground state $|1\rangle$ and excited state $|0\rangle$ as

$$|\psi(0)\rangle = e^{-i\theta J_x^2/2} |1\rangle^{\otimes N} \equiv e^{-i\theta J_x^2/2} |1\rangle, \quad (8)$$

where N is the number of the total qubits, the Hamiltonian is $H = \chi J_x^2$, χ is the coupling constant and $\theta = 2\chi t$ is the twist angle. By setting the mean spin of the initial state along the z direction, the two-qubit reduced density matrix becomes [51]

$$\rho_{AB}(0) = \begin{pmatrix} \delta_+ & 0 & 0 & \gamma^* \\ 0 & \mu & \tau & 0 \\ 0 & \tau & \mu & 0 \\ \gamma & 0 & 0 & \delta_- \end{pmatrix}, \quad (9)$$

in the basis $\{|11\rangle, |00\rangle, |01\rangle, |10\rangle\}$, where

$$\begin{aligned} \delta_{\pm} &= (1 \pm 2\langle\hat{\sigma}_{1z}\rangle + \langle\hat{\sigma}_{1z}\hat{\sigma}_{2z}\rangle)/4, \\ \mu &= (1 - \langle\hat{\sigma}_{1z}\hat{\sigma}_{2z}\rangle)/4, \\ \tau &= \langle\hat{\sigma}_{1+}\hat{\sigma}_{2-}\rangle, \\ \gamma &= \langle\hat{\sigma}_{1-}\hat{\sigma}_{2-}\rangle \end{aligned} \quad (10)$$

with $\langle\hat{\sigma}_z\rangle = -\cos^{N-1}(\frac{\theta}{2})$, $\langle\hat{\sigma}_{1z}\hat{\sigma}_{2z}\rangle = (1 + \cos^{N-2}\theta)/2$, $\langle\hat{\sigma}_{1+}\hat{\sigma}_{2-}\rangle = \frac{1}{8}(1 - \cos^{N-2}\theta)$, $\langle\hat{\sigma}_{1-}\hat{\sigma}_{2-}\rangle = -\frac{1}{8}(1 - \cos^{N-2}\theta) - \frac{i}{2}\sin(\frac{\theta}{2})\cos^{N-2}(\frac{\theta}{2})$. Then, we choose the standard one-axis twisted state as the initial state under the dephasing channels where the probes are only coupled to their own baths. As a result, the total Hamiltonian can be written as

$$H_I = \sum_{l=1}^N (H_{0,l} \otimes I_{2 \times 2} + \eta H_{1,l} \otimes \hat{\sigma}_{l,z}), \quad (11)$$

and the unitary matrix can be obtained as

$$\begin{aligned} U_I &= e^{-iH_I t} = \prod_{l=1}^N U_l \\ &= \prod_{l=1}^N e^{-iH_{0,l} t} e^{-i\eta \hat{\sigma}_{l,z} H_{1,l} t}, \end{aligned} \quad (12)$$

where $H_{0,l}$ and $H_{1,l}$ denote the Hamiltonian of the l -th environment and the l -th random field, respectively. The probe spin lying in the bath is coupled to all the N_b bath spins equally. Besides, it is known that the evolution of any finite number of particles is governed only by the local Hamiltonian of the particles and their baths, we hence attain the time evolution density matrix of the system

$$\rho(t) = U [\rho_E(0) \otimes \rho_{AB}(0)] U^\dagger, \quad (13)$$

by employing the unitary transformation, where $\rho_E(0)$

and $\rho_{AB}(0)$ are the initial density matrices of the environment and the spin, respectively. Thus, we have the system's final state as

$$\rho_{IAB}(t) = \begin{pmatrix} \delta_+ & 0 & 0 & P_+^2 \gamma^* \\ 0 & \mu & P_+ P_- \tau & 0 \\ 0 & P_+ P_- \tau & \mu & 0 \\ P_-^2 \gamma & 0 & 0 & \delta_- \end{pmatrix}, \quad (14)$$

where

$$P_{\pm} = \frac{Z(\beta, h \pm 2i\eta t/\beta)}{Z(\beta, h)} = \frac{e^{2iN_b \eta t} \prod_{n=1}^{N_b} (e^{-2\beta(h \pm 2i\eta t/\beta)} - z_n)}{\prod_{n=1}^{N_b} (e^{-2\beta h} - z_n)} \quad (15)$$

is the analogous partition function. If we consider the probe coupled to a ferromagnetic Ising bath under zero field ($h = 0$), one can verify that the analogous partition function is with form of

$$P(ix) = \frac{e^{i\beta N_b x} \prod_{n=1}^{N_b} (e^{-2i\beta x} - e^{i\phi_n})}{\prod_{n=1}^{N_b} (1 - e^{i\phi_n})}, \quad (16)$$

where the real number $x = \pm 2\eta t/\beta$, implying $P^*(ix) = P(-ix)$ is hold. Therefore, we have

$$\rho_{IAB}(t) = \begin{pmatrix} \delta_+ & 0 & 0 & P^2 \gamma^* \\ 0 & \mu & P^2 \tau & 0 \\ 0 & P^2 \tau & \mu & 0 \\ P^2 \gamma & 0 & 0 & \delta_- \end{pmatrix} \quad (17)$$

in the basis of $\{|11\rangle, |00\rangle, |01\rangle, |10\rangle\}$ [52]. Furthermore, the three Kraus operators can be given by

$$\begin{aligned} M_0 &= \sqrt{P^2} I, \\ M_1 &= \sqrt{1 - P^2} |0\rangle\langle 0|, \\ M_2 &= \sqrt{1 - P^2} |1\rangle\langle 1|, \end{aligned} \quad (18)$$

where I is the identity operator.

Next, we introduce the other dephasing channel where N probes are coupled to one N_b spins together. In such scenarios, the total Hamiltonian is written as

$$H_{II} = H_0 \otimes I_{2N \times 2N} + \eta H_1 \otimes \sum_{l=1}^N \hat{\sigma}_{l,z}, \quad (19)$$

and the unitary matrix is

$$U_{II} = e^{-iH_{II}t} = e^{-iH_0 t} e^{-i\eta \sum_{j=1}^N \hat{\sigma}_{l,z} H_1 t}. \quad (20)$$

By choosing the one-axis twisted state as the initial state, we have the evolution of the reduced initial state as

$$\rho_{IIAB}(t) = \begin{pmatrix} \delta_+ & 0 & 0 & P' \gamma^* \\ 0 & \mu & \tau & 0 \\ 0 & \tau & \mu & 0 \\ P' \gamma & 0 & 0 & \delta_- \end{pmatrix}. \quad (21)$$

Here we consider the system under zero field ($h = 0$), where $P' = P(\pm 4i\eta t/\beta)$. In such a dephasing channel, the Kraus operators can be derived as

$$\begin{aligned} M_0 &= \sqrt{1 - P'} |00\rangle\langle 00|, \\ M_1 &= \sqrt{1 - P'} |11\rangle\langle 11|, \\ M_2 &= \sqrt{P'} (|00\rangle\langle 00| + |11\rangle\langle 11|), \\ M_3 &= |01\rangle\langle 01| + |10\rangle\langle 10|. \end{aligned} \quad (22)$$

3 The dynamics of the uncertainty under Lee–Yang dephasing channels

To expose the dynamical characteristic of the measurements uncertainty of interest in the current scenario, we herein utilize a pair of Pauli operators $\hat{\sigma}_x$ and $\hat{\sigma}_z$ as the incompatibility. Hence, associated with the final state in Eq. (14), the post-measurement states can be described as

$$\begin{aligned} \rho_{\hat{\sigma}_x B}(t) &= \frac{\delta_+ + \mu}{2} (|00\rangle\langle 00| + |10\rangle\langle 10|) \\ &\quad + \frac{\delta_- + \mu}{2} (|01\rangle\langle 01| + |11\rangle\langle 11|) \\ &\quad + \frac{1}{2} (P^2 \tau + P^2 \gamma^*) (|00\rangle\langle 11| + |10\rangle\langle 01|) \\ &\quad + \frac{1}{2} (P^2 \gamma + P^2 \tau) (|01\rangle\langle 10| + |11\rangle\langle 00|) \end{aligned} \quad (23)$$

and

$$\begin{aligned} \rho_{\hat{\sigma}_z B}(t) &= \delta_+ |00\rangle\langle 00| + \mu |01\rangle\langle 01| \\ &\quad + \mu |10\rangle\langle 10| + \delta_- |11\rangle\langle 11|. \end{aligned} \quad (24)$$

Consequently, one can easily obtain the states' eigenvalues and give rise to the von Neumann entropies $H(\rho) = -\sum_i \lambda_i \log_2 \lambda_i$ with $\lambda_1^{\hat{\sigma}_x} = \lambda_2^{\hat{\sigma}_x} = \frac{1}{8} (2 - \sqrt{1 + P^4})$, $\lambda_3^{\hat{\sigma}_x} = \lambda_4^{\hat{\sigma}_x} = \frac{1}{8} (2 + \sqrt{1 + P^4})$ and $\lambda_1^{\hat{\sigma}_z} = \frac{5}{8}, \lambda_2^{\hat{\sigma}_z} = \lambda_3^{\hat{\sigma}_z} = \lambda_4^{\hat{\sigma}_z} = \frac{1}{8}$ when $N = 3$ and $\theta = \pi/2$.

Because the Lee–Yang zeros (z_n) only depend on the particle number (N_b) and the temperature (β or $1/T$). We choose the 1D Ising model with $N_b = 10$ at infinite temperature ($\beta = 0$) in order that all the Lee–Yang zeros have degenerated at $z_n = -1$.

It is worth noting that we focus on investigating the dynamics of uncertainty in the quantum dephasing channel where probes are coupled to their own baths. In Fig. 2, we draw the entropic uncertainty as a function of the dephasing channel strength P^2 . It can be clearly found that the uncertainty decreases with the increase of strength, and its dynamic shows a monotonic behavior. In addition, we also show the evolution of the systemic

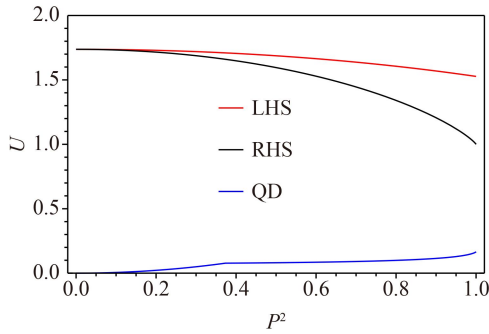


Fig. 2 QMA entropic uncertainty, the lower bounds and quantum discord (QD) as a function of the dephasing strength in the case of qubit A passing through the dephasing channel where probes are coupled to their own baths, and keep B as a quantum memory. $N = 3$ and $\theta = \pi/2$. Here, LHS denotes the left-hand side of Eq. (3), RHS denotes the right-hand side of the inequality, QD represents quantum discord of A and B .

quantum correlation, quantified by quantum discord (QD) [53, 54], one can see that the variation of the QD is almost opposite to the variation of the EUR, however, when P^2 is close to 0.4, the variation of the EUR is not fully opposite to the QD of the system. To explain the relationship between EUR and QD, we resort to the conditional entropy of the system as $H_{\{\Pi_i^B\}}(\rho_{A|B})$. In general, the QD of a bipartite composite system can be written as

$$Q(\rho_{AB}) = I(A : B) - C(\rho_{AB}), \tag{25}$$

where the mutual information $I(A : B)$ represents the overall correlation for A and B , which can be obtained as

$$I(A : B) = H(\rho_A) + H(\rho_B) - H(\rho_{AB}), \tag{26}$$

and $C(\rho_{AB})$ indicates the classical correlation related to A and B , which can be described as

$$C(\rho_{AB}) = \max_{\{\Pi_i^B\}} \left[H(\rho_A) - H_{\{\Pi_i^B\}}(\rho_{A|B}) \right]. \tag{27}$$

Combining Eqs. (3), (26) and (27), we have

$$U_R = -Q(\rho_{AB}) + H_{\{\Pi_i^B\}}(\rho_{A|B}) + \log \frac{1}{c}, \tag{28}$$

where c is an overlap, and here it is a constant. upon the result (28), we offer the reason that the uncertainty is not fully anti-correlated with the QD as: (i) the dynamics of the bound are determined by two primary elements, i.e., the quantum correlation $Q(\rho_{AB})$ and the conditional entropy $H_{\{\Pi_i^B\}}(\rho_{A|B})$; (ii) there is natural competition between QD of the system and the conditional entropy $H_{\{\Pi_i^B\}}(\rho_{A|B})$.

Besides, we show the relationship between the Lee–Yang zeros and the entropic uncertainty relations of

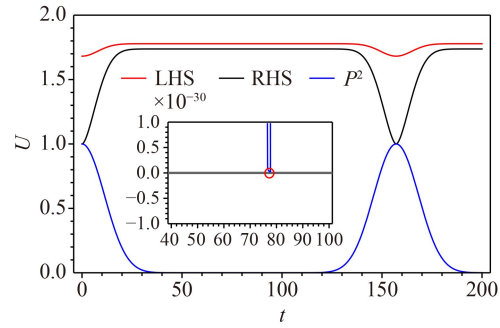


Fig. 3 The relationship between the Lee–Yang zeros, the entropic uncertainty and the lower bounds of the probes coupled to their own baths, LHS for the red line, RHS for the black line and the analogous partition function P^2 for the blue line.

the probes coupled to their own bath, as shown in Fig. 3. Notably, the analogous partition function is anti-correlated with the uncertainty, which corresponds to the result obtained before. Besides, in order to reveal how the environment affects the dynamics of the uncertainty, we also take the measurement uncertainty as a function of evolution time t in Fig. 3. Following the figure, the uncertainty has a periodic dynamical behavior, and the uncertainty is always no lower than the initial value. Besides, the uncertainty will saturate into a fixed maximum in a fixed long-time limit.

Next, let us turn to the effect of the twisted angle on the uncertainty of interest. As plotted in Fig. 4, the uncertainty increases with the increasing twisted angle θ from $\pi/4$ to $\pi/2$ in Fig. 4(a). Similarly, the larger N can induce the greater uncertainty, as indicated in Fig. 4(b).

As mentioned above, we have explored the dynamic relationship of the uncertainty under the first type of Lee–Yang dephasing channel. Next, we will continue to exploit the dynamics of the uncertainty under the other type of Lee–Yang dephasing channel where N probes are coupled to one bath together. It is found that, with the increase of dephasing channel strength, the uncertainty presents monotonicity and gradually decreases, as shown in Fig. 5. Also, the changing trend of QD is not fully anti-correlated with uncertainty. This is because the magnitude of uncertainty’s bound is determined by both QD and the conditional entropy $H_{\{\Pi_i^B\}}(\rho_{A|B})$, which exhibit the natural competition while quantifying the uncertainty.

Notably, we find that the uncertainty is inversely correlated with the class partition function P' . Numerically, we plot the dynamics of the uncertainty, its bound and P' as a function of time t in Fig. 6. Following the figure, the uncertainty will inflate and tend to a stable value, and the partition function will decrease and saturate into zero with the increasing time. In Fig. 7, it is easy to know that the quantum correlation decreases and the uncertainty increase when the twisted angle θ and the

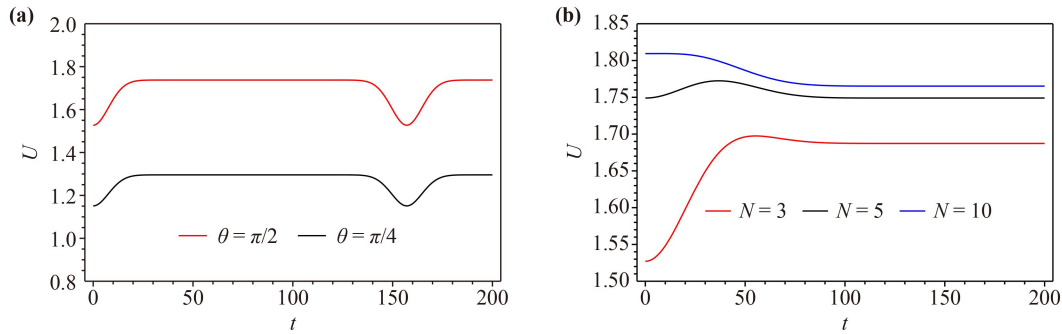


Fig. 4 Entropic uncertainty with the change of t under the infinite temperature ($\beta = 0$) in the case of qubit A passing through the dephasing channel where probes are coupled to their own baths. **(a)** The number of the probes $N = 3$ and the twist angle $\theta = \pi/2$ for the red line, $\theta = \pi/4$ for the black line. **(b)** $N = 3$ for the red line, $N = 5$ for the blue line, $N = 10$ for the black line under $\theta = \pi/2$. The probes-bath coupling constant is $\eta = 0.01$.

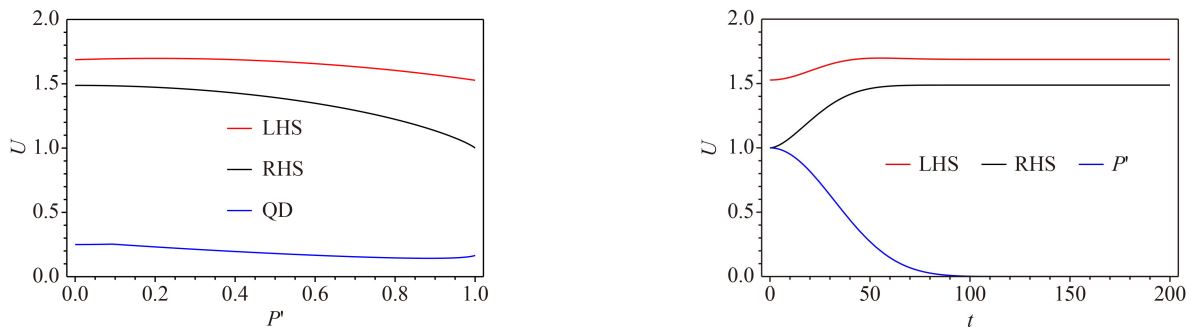


Fig. 5 Entropic uncertainty, the lower bounds and QD as a function of the dephasing strength in the case of qubit A passing through the dephasing channel where N probes are coupled to one bath together, and keep B as a quantum memory. $N = 3$ and $\theta = \pi/2$. Here, LHS denotes the left-hand side of Eq. (3), while RHS denotes the right-hand side of the inequality. QD represents quantum discord of A and B .

probes number N are increased. In conclusion, it is clear to know that the dynamic characteristics of the uncertainty under the two dephasing channels are almost identical.

4 Manipulating the entropic uncertainty by using the \mathcal{PT} -symmetric operation

Generally, quantum systems inevitably interact with their surrounding environment, resulting in quantum decoherence or quantum dissipation effects. Therefore, how to suppress the decoherence effect is of great significance in practical quantum information processing and communication. Pourkarimi *et al.* [55] found that the entropic uncertainty decreases in specific channels such as phase-flip (PF) and amplitude damping (AD) channels. Herein, it is different from the work by Pourkarimi *et al.* [55], we would like to introduce an efficient method – parity–time–symmetric (\mathcal{PT} -symmetric) opera-

Fig. 6 The relationship between the Lee–Yang zeros, entropic uncertainty and the lower bounds of the probes coupled to own bath together, LHS for the red line, RHS for the black line and the analogous partition function P' for the blue line.

tions – which can be utilized for reducing the entropic uncertainty.

The known \mathcal{PT} -symmetric Hamiltonian was proposed by Bender *et al.* [56, 57]. There is something supposed to be further explained, \mathcal{P} is the parity reflection operator and \mathcal{T} is the time reversal operator. The \mathcal{PT} -symmetric Hamiltonian for a particle can be expressed as [58]

$$\mathcal{H} = s \begin{pmatrix} i \sin \alpha & 1 \\ 1 & -i \sin \alpha \end{pmatrix}, \quad (29)$$

where angle $\alpha \in (-\pi/2, \pi/2)$ denotes the non-Hermiticity of the Hamiltonian and s is a general scaling constant of the matrix. The time-evolution operator for \mathcal{H} is given by

$$U(t) = e^{-i\mathcal{H}t} = \frac{1}{\cos \alpha} \begin{pmatrix} \cos(t' - \alpha) & -i \sin t' \\ -i \sin t' & \cos(t' + \alpha) \end{pmatrix}, \quad (30)$$

where $t' = \Delta E t/2$, $\Delta E = E_+ - E_-$, E_{\pm} are the eigenvalues of \mathcal{H} , and $E_{\pm} = \pm s \cos \alpha$. In the following, we will elaborate

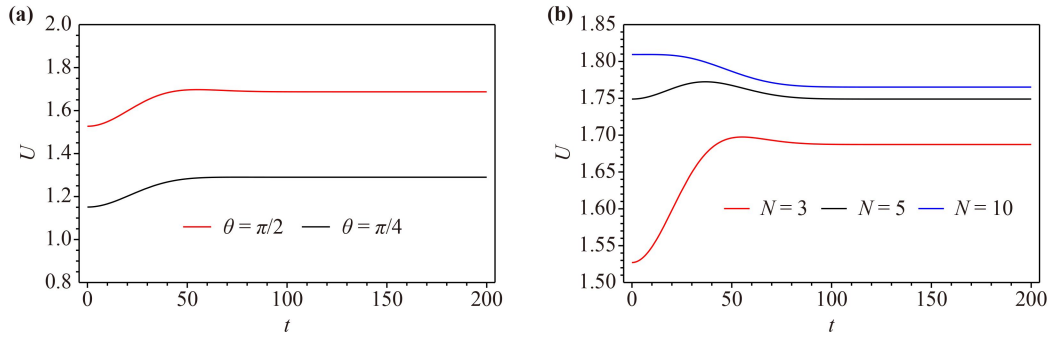


Fig. 7 Entropic uncertainty with the change of t under the infinite temperature ($\beta = 0$) in the case of qubit A passing through the dephasing channel where probes are coupled to one bath together. **(a)** $N = 3$ and $\theta = \pi/2$ for the red line, $\theta = \pi/4$ for the black line. **(b)** $N = 3$ for the red line, $N = 5$ for the blue line, $N = 10$ for the black line under $\theta = \pi/2$. The probes-bath coupling constant is $\eta = 0.01$.

on how to manipulate the uncertainty in the two kinds of dephasing channels by virtue of \mathcal{PT} -symmetric operations.

4.1 Reduction of entropic uncertainty by a local \mathcal{PT} -symmetric operation under dephasing channels where probes are coupled to their own baths

Considering qubit A goes through the dephasing channel and keeping B as a quantum memory. Then, after qubit A goes through the dephasing channel we perform a local \mathcal{PT} -symmetric operation on it. By using the time-evolution operator in Eq. (30), the final state of the system can be given as

$$\rho_{t'} = \frac{[U(t) \otimes I] \rho_t [U(t) \otimes I_B]^\dagger}{\text{Tr} [(U(t) \otimes I_B) \rho_t (U(t) \otimes I_B)^\dagger]} \quad (31)$$

Without loss of generality, we also resort to the Pauli operators for measurements to evaluate the performance of the QMA entropic uncertainty. As a result, the post-measurement state of the system can be given as

$$\begin{aligned} \rho_{\hat{\sigma}_x B} &= \sum_i (|\hat{\sigma}_{xi}\rangle \langle \hat{\sigma}_{xi}| \otimes I_B) \rho_t (|\hat{\sigma}_{xi}\rangle \langle \hat{\sigma}_{xi}| \otimes I_B), \\ \rho_{\hat{\sigma}_z B} &= \sum_j (|\hat{\sigma}_{zj}\rangle \langle \hat{\sigma}_{zj}| \otimes I_B) \rho_t (|\hat{\sigma}_{zj}\rangle \langle \hat{\sigma}_{zj}| \otimes I_B), \end{aligned} \quad (32)$$

after making the operation on qubit A , where $\{|\hat{\sigma}_{xi}\rangle\}$ and $\{|\hat{\sigma}_{zj}\rangle\}$ are the eigenstates of a pair of incompatible observables $\hat{\sigma}_x$ and $\hat{\sigma}_z$.

In Fig. 8, we plot the dynamics of the QMA entropic uncertainty under the \mathcal{PT} -symmetric operation, one could reveal that how powerful the \mathcal{PT} -symmetric operation reduces the uncertainty. We first consider the different parameters N in Fig. 8(a). It is shown that the uncertainty changes periodically with the increase of interaction time, especially, the reduction degree reaches the maximum in a certain time. It can be clearly seen that the smaller N can induce the reduction of the uncertainty magnitude under \mathcal{PT} -symmetric operation. In order to further attain the influence of the \mathcal{PT} -symmetric operation on uncertainty, we draw the uncertainty as a function of time with \mathcal{PT} -symmetric operation and without the operation respectively in Fig. 8(b), and we find that at a certain time interval, the uncertainty

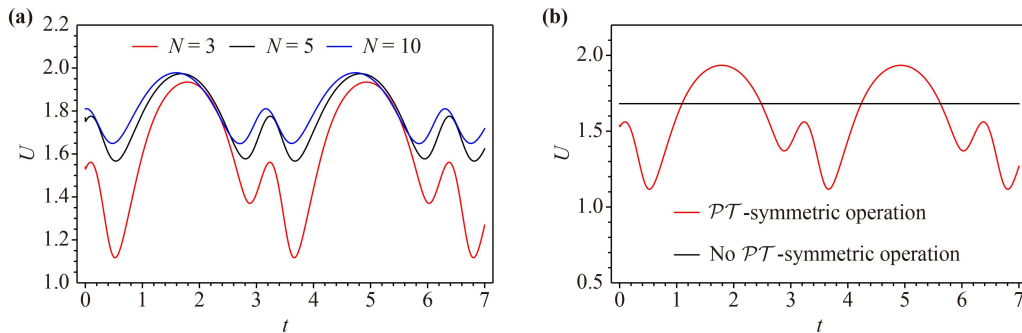


Fig. 8 QMA entropic uncertainty under the local \mathcal{PT} -symmetric operation with the change of t where probes are coupled to their own baths, $N = 3$ for the red line, $N = 5$ for the blue line, $N = 10$ for the black line. All plotted with $\alpha = \frac{\pi}{4}$ and $\theta = \pi/2$.

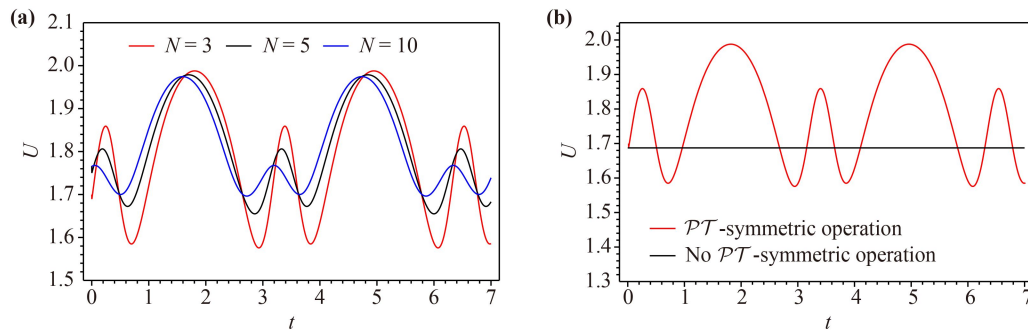


Fig. 9 QMA entropic uncertainty under the local \mathcal{PT} -symmetric operation with the change of t where probes are coupled to one bath together, $N = 3$ for the red line, $N = 5$ for the blue line, $N = 10$ for the black line. All plotted with $\alpha = \frac{\pi}{4}$ and $\theta = \pi/2$.

decreases with the operation time. In this sense, we believe that the \mathcal{PT} -symmetric operation can effectively reduce the entropy uncertainty by modulating the operation time, which is virtually required in practical quantum information processing.

4.2 Reduction of entropic uncertainty by a local \mathcal{PT} -symmetric operation under dephasing channels where the probes are coupled to one bath collectively

Technically, we here consider that qubit A is affected by the dephasing channel and keeping qubit B as a quantum memory. And the local \mathcal{PT} -symmetric operation is performed on particle A . In order to gain the influence of the operation on uncertainty, we plot the change of entropic uncertainty with time in Fig. 9 when $P = 0$ and N is different. It is clear that at a certain time interval, the uncertainty decreases with the operation time. In (a) when $N = 3$, the uncertainty decreases most obviously. While (b) shows the cases with or without \mathcal{PT} -symmetric operation for comparison. According to the numeric result, one can conjecture that the \mathcal{PT} -symmetric operation is able to effectively reduce the entropic uncertainty in a specific time period. With this in consideration, appropriate control of interaction time is crucial to reduce the uncertainty in reality. In addition, the final state under this channel is the same as that under the first channel when $P = 0$. By comparison, one can find that the intensity of dephasing channel plays a positive role in reducing the entropic uncertainty under the \mathcal{PT} -symmetric operation.

5 Conclusion

To conclude, we have investigated the measured uncertainty when the subsystem to be measured passes through two different types of Lee–Yang dephasing channels respectively, one is that the probes are coupled to their own bath and the other is that the probes are coupled to one bath together. It turns out that the two different types of Lee–Yang dephasing channels can give

rise to a negative impact on the entropic uncertainty, and the magnitude of uncertainty is related to the number of the probes and the twist angle. Then, we have put forward a working method to manipulate the amount of the measured uncertainty, and to a certain extent, the uncertainty of measurement can be reduced by properly modulating the \mathcal{PT} -symmetry operations under both channels. Besides, we render a physical interpretation concerning those phenomena of the uncertainty dynamics: the evolution of the measured uncertainty is not only dependent on the QD of the system, but the conditional von Neumann entropy of the measured subsystem. More importantly, the analogous partition function is anti-correlated with the uncertainty. We believe our exploration would be beneficial to insight into the uncertainty dynamics under decoherence, and be of basic importance in measurement-based quantum information processing.

Acknowledgements This study was supported by the National Natural Science Foundation of China (Grant Nos. 12075001 and 12175001), Anhui Provincial Key Research and Development Plan (Grant No. 2022b13020004), Anhui Provincial Natural Science Foundation (Grant No. 1508085QF139), and the Fund of the CAS Key Laboratory of Quantum Information (Grant No. KQI201701).

References

1. W. Heisenberg, Über den anschaulichen Inhalt der quantentheoretischen kinematik und mechanik, *Eur. Phys. J. A* 43(3–4), 172 (1927)
2. E. H. Kennard, Zur quantenmechanik einfacher bewegungstypen, *Eur. Phys. J. A* 44(4–5), 326 (1927)
3. H. P. Robertson, The uncertainty principle, *Phys. Rev.* 34(1), 163 (1929)
4. H. Maassen and J. B. M. Uffink, Generalized entropic uncertainty relations, *Phys. Rev. Lett.* 60(12), 1103 (1988)
5. I. Białyński-Birula and J. Mycielski, Uncertainty relations for information entropy in wave mechanics, *Commun. Math. Phys.* 44(2), 129 (1975)



6. D. Deutsch, Uncertainty in quantum measurements, *Phys. Rev. Lett.* 50(9), 631 (1983)
7. K. Kraus, Complementary observables and uncertainty relations, *Phys. Rev. D* 35(10), 3070 (1987)
8. J. M. Renes and J. C. Boileau, Conjectured strong complementary information tradeoff, *Phys. Rev. Lett.* 103(2), 020402 (2009)
9. M. Berta, M. Christandl, R. Colbeck, J. M. Renes, and R. Renner, The uncertainty principle in the presence of quantum memory, *Nat. Phys.* 6(9), 659 (2010)
10. C. F. Li, J. S. Xu, X. Y. Xu, K. Li, and G. C. Guo, Experimental investigation of the entanglement-assisted entropic uncertainty principle, *Nat. Phys.* 7(10), 752 (2011)
11. L. J. Li, F. Ming, X. K. Song, L. Ye, and D. Wang, Review on entropic uncertainty relations, *Acta Physica Sinica* 71(7), 070302 (2022)
12. M. Tomamichel and R. Renner, Uncertainty relation for smooth entropies, *Phys. Rev. Lett.* 106(11), 110506 (2011)
13. P. J. Coles, R. Colbeck, L. Yu, and M. Zwolek, Uncertainty relations from simple entropic properties, *Phys. Rev. Lett.* 108(21), 210405 (2012)
14. J. Zhang, Y. Zhang, and C. S. Yu, Rényi entropy uncertainty relation for successive projective measurements, *Quantum Inform. Process.* 14(6), 2239 (2015)
15. J. Schneeloch, C. J. Broadbent, S. P. Walborn, E. G. Cavalcanti, and J. C. Howell, Einstein–Podolsky–Rosen steering inequalities from entropic uncertainty relations, *Phys. Rev. A* 87(6), 062103 (2013)
16. M. L. Hu and H. Fan, Quantum-memory-assisted entropic uncertainty principle, teleportation, and entanglement witness in structured reservoirs, *Phys. Rev. A* 86(3), 032338 (2012)
17. M. L. Hu and H. Fan, Competition between quantum correlations in the quantum-memory-assisted entropic uncertainty relation, *Phys. Rev. A* 87(2), 022314 (2013)
18. M. L. Hu and H. Fan, Upper bound and shareability of quantum discord based on entropic uncertainty relations, *Phys. Rev. A* 88(1), 014105 (2013)
19. A. K. Pati, M. M. Wilde, A. R. U. Devi, A. K. Rajagopal, and Sudha, Quantum discord and classical correlation can tighten the uncertainty principle in the presence of quantum memory, *Phys. Rev. A* 86(4), 042105 (2012)
20. J. Zhang, Y. Zhang, and C. S. Yu, Entropic uncertainty relation and information exclusion relation for multiple measurements in the presence of quantum memory, *Sci. Rep.* 5(1), 11701 (2015)
21. S. Liu, L. Z. Mu, and H. Fan, Entropic uncertainty relations for multiple measurements, *Phys. Rev. A* 91(4), 042133 (2015)
22. F. Adabi, S. Salimi, and S. Haseli, Tightening the entropic uncertainty bound in the presence of quantum memory, *Phys. Rev. A* 93(6), 062123 (2016)
23. F. Adabi, S. Haseli, and S. Salimi, Reducing the entropic uncertainty lower bound in the presence of quantum memory via LOCC, *Europhys. Lett.* 115(6), 60004 (2016)
24. A. E. Rastegin and K. Zyczkowski, Majorization entropic uncertainty relations for quantum operations, *J. Phys. A Math. Theor.* 49(35), 355301 (2016)
25. D. Wang, A. J. Huang, R. D. Hoehn, F. Ming, W. Y. Sun, J. D. Shi, L. Ye, and S. Kais, Entropic uncertainty relations for Markovian and non-Markovian processes under a structured bosonic reservoir, *Sci. Rep.* 7(1), 1066 (2017)
26. K. Baek and W. Son, Unsharpness of generalized measurement and its effects in entropic uncertainty relations, *Sci. Rep.* 6(1), 30228 (2016)
27. M. Berta, S. Wehner, and M. M. Wilde, Entropic uncertainty and measurement reversibility, *New J. Phys.* 18(7), 073004 (2016)
28. Y. Y. Yang, W. Y. Sun, W. N. Shi, F. Ming, D. Wang, and L. Ye, Dynamical characteristic of measurement uncertainty under Heisenberg spin models with Dzyaloshinskii–Moriya interactions, *Front. Phys.* 14(3), 31601 (2019)
29. D. Wang, F. Ming, M. L. Hu, and L. Ye, Quantum-memory-assisted entropic uncertainty relations, *Ann. Phys.* 531(10), 1900124 (2019)
30. F. Ming, D. Wang, X. G. Fan, W. N. Shi, L. Ye, and J. L. Chen, Improved tripartite uncertainty relation with quantum memory, *Phys. Rev. A* 102(1), 012206 (2020)
31. B. F. Xie, D. Wang, L. Ye, and J. L. Chen, Optimized entropic uncertainty relations for multiple measurements, *Phys. Rev. A* 104(6), 062204 (2021)
32. L. Wu, L. Ye, and D. Wang, Tighter generalized entropic uncertainty relations in multipartite systems, *Phys. Rev. A* 106(6), 062219 (2022)
33. Z. A. Wang, B. F. Xie, F. Ming, Y. T. Wang, D. Wang, Y. Meng, Z. H. Liu, J. S. Tang, L. Ye, C. F. Li, G. C. Guo, and S. Kais, Generalized multipartite entropic uncertainty relations: Theory and experiment, arXiv: 2207.12693 (2022)
34. L. Y. Cheng, F. Ming, F. Zhao, L. Ye, and D. Wang, The uncertainty and quantum correlation of measurement in double quantum-dot systems, *Front. Phys.* 17(6), 61504 (2022)
35. L. J. Li, F. Ming, X. K. Song, L. Ye, and D. Wang, Quantumness and entropic uncertainty in curved spacetime, *Eur. Phys. J. C* 82(8), 726 (2022)
36. M. L. Song, L. J. Li, X. K. Song, L. Ye, and D. Wang, Environment-mediated entropic uncertainty in charging quantum batteries, *Phys. Rev. E* 106(5), 054107 (2022)
37. M. R. Pourkarimi and S. Haddadi, Quantum-memory-assisted entropic uncertainty, teleportation, and quantum discord under decohering environments, *Laser Phys. Lett.* 17(2), 025206 (2020)
38. F. Benabdallah, A. U. Rahman, S. Haddadi, and M. Daoud, Long-time protection of thermal correlations in a hybrid-spin system under random telegraph noise, *Phys. Rev. E* 106(3), 034122 (2022)
39. M. R. Pourkarimi, S. Haseli, S. Haddadi, and M. Hadipour, Scrutinizing entropic uncertainty and quantum discord in an open system under quantum critical environment, *Laser Phys. Lett.* 19(6), 065201 (2022)
40. S. Haddadi, M. L. Hu, Y. Khedif, H. Dolatkah, M. R. Pourkarimi, and M. Daoud, Measurement uncertainty and dense coding in a two-qubit system: Combined effects of bosonic reservoir and dipole–dipole interaction, *Results Phys.* 32, 105041 (2022)

41. G. Vallone, D. G. Marangon, M. Tomasin, and P. Villoresi, Quantum randomness certified by the uncertainty principle, *Phys. Rev. A* 90(5), 052327 (2014)
42. C. N. Yang and T. D. Lee, Statistical theory of equations of state and phase transitions. I. Theory of condensation, *Phys. Rev.* 87(3), 404 (1952)
43. T. D. Lee and C. N. Yang, Statistical theory of equations of state and phase transitions. II. Lattice gas and Ising model, *Phys. Rev.* 87(3), 410 (1952)
44. M. E. Fisher, Yang–Lee edge singularity and ϕ^3 field theory, *Phys. Rev. Lett.* 40(25), 1610 (1978)
45. P. J. Kortman and R. B. Griffiths, Density of zeros on the Lee–Yang circle for two Ising ferromagnets, *Phys. Rev. Lett.* 27(21), 1439 (1971)
46. B. B. Wei and R. B. Liu, Lee–Yang zeros and critical times in decoherence of a probe spin coupled to a bath, *Phys. Rev. Lett.* 109(18), 185701 (2012)
47. M. Schlosshauer, Decoherence, the measurement problem, and interpretations of quantum mechanics, *Rev. Mod. Phys.* 76(4), 1267 (2005)
48. R. B. Liu, W. Yao, and L. J. Sham, Control of electron spin decoherence caused by electron–nuclear spin dynamics in a quantum dot, *New J. Phys.* 9(7), 226 (2007)
49. I. Białynicki-Birula, Rényi entropy and the uncertainty relations, *AIP Conf. Proc.* 889, 52 (2007)
50. Y. G. Su, H. B. Liang, and X. G. Wang, Spin squeezing and concurrence under Lee–Yang dephasing channels, *Phys. Rev. A* 102(5), 052423 (2020)
51. X. Yin, J. Ma, X. Wang, and F. Nori, Spin squeezing under non-Markovian channels by the hierarchy equation method, *Phys. Rev. A* 86(1), 012308 (2012)
52. X. Wang and B. C. Sanders, Spin squeezing and pairwise entanglement for symmetric multiqubit states, *Phys. Rev. A* 68(1), 012101 (2003)
53. J. L. Chen, C. L. Ren, C. B. Chen, X. J. Ye, and A. K. Pati, Bell’s nonlocality can be detected by the violation of Einstein–Podolsky–Rosen steering inequality, *Sci. Rep.* 6(1), 39063 (2016)
54. K. Sun, X. J. Ye, J. S. Xu, X. Y. Xu, J. S. Tang, Y. C. Wu, J. L. Chen, C. F. Li, and G. C. Guo, Experimental quantification of asymmetric Einstein–Podolsky–Rosen steering, *Phys. Rev. Lett.* 116(16), 160404 (2016)
55. M. R. Pourkarimi, S. Haddadi, and S. Haseli, Exploration of entropic uncertainty bound in a symmetric multiqubit system under noisy channels, *Phys. Scr.* 96(1), 015101 (2020)
56. C. M. Bender and S. Boettcher, Real spectra in non-Hermitian Hamiltonians having PT symmetry, *Phys. Rev. Lett.* 80(24), 5243 (1998)
57. C. M. Bender, D. C. Brody, and H. F. Jones, Complex extension of quantum mechanics, *Phys. Rev. Lett.* 89(27), 270401 (2002)
58. U. Günther and B. F. Samsonov, Naimark-dilated PT -symmetric brachistochrone, *Phys. Rev. Lett.* 101(23), 230404 (2008)